Shrinking Kinetics of Polyacrylate Gels in Surfactant Solution

Anders Göransson and Per Hansson*

Pharmaceutical Physical Chemistry, Department of Pharmacy, Uppsala University, P.O. Box 580, S-75123 Uppsala, Sweden

Received: November 29, 2002; In Final Form: June 12, 2003

Volume transition of covalently cross-linked sodium polyacrylate gels (micrometer-sized) due to the absorption of dodecyltrimethylammonium bromide from bulk aqueous solution is studied by means of light and fluorescence microscopy. The volume transition occurs in a narrow range of surfactant concentrations. In the presence of 0.01 M sodium bromide in the solution, the equilibrium volume is reduced typically 50 times for surfactant concentrations larger that 4×10^{-4} M. During the transition, a collapsed, surfactant-rich, surface phase is formed, enclosing the swollen gel core. Evidence is found for equilibrium between the core and surface phase in the collapsed state of the gel. The relation to surfactant self-assembly in solutions of linear polyion and in centimeter-sized gels is discussed. The kinetics of diffusion-controlled shrinking is analyzed theoretically. The model considers the transport of surfactant from the bulk, through the "stagnant" liquid layer and the surface phase, to the gel core. During shrinking, the osmotic swelling of the gel is assumed to be in quasi-equilibrium with the bulk and calculated using a recent model for equilibrium swelling of phase-separated gels (Hansson et al. *J. Phys. Chem. B* **2002**, *106*, 9777). The kinetic model is used to analyze time-resolved experimental shrinking curves. The result suggests that the shrinking is controlled by stagnant layer diffusion of surfactant, and that the relative swelling at intermediate stages during the collapse is the same as for slab gels of the same composition. The lag time measured before shrinking starts is longer than the time expected for the surfactant concentration to exceed the critical aggregation concentration in the gels, suggesting that the gels are arrested for some time in a metastable state before the surface phase starts to form.

Introduction

Polyelectrolyte networks undergo a large swelling when placed in water.[1] The swelling is an osmotic effect mainly due to the presence of network counterions.[2] The swelling can be reduced in different ways, for instance, by adding salt to the solution, changing the solvent,[3] or applying an external electric field.[4] Often the effect is dramatic, characterized by a discrete volume (or phase) transition.[5−7] The macroscopic response reflects processes taking place on the level of individual chains in the network. For instance, the discrete coil−globule transition of individual DNA chains taking place in a 60/40 acetone/water mixture, evident from recent fluorescence microscopy studies,[8] has its macroscopic counterpart in the sharp volume transition of covalently cross-linked DNA gels at the same composition of the solvent.[9]

Charged networks play an important role in specialized secretory cells as constituents of "granules" (secretory vesicles) with the function of concentrating and storing large amounts of substances, e.g., histamine.[10−13] This is possible since the (proteoglycan) networks can absorb large amounts of oppositely charged species, making storage in a small volume possible. Attempts have been made to mimic this for drug delivery purposes.[14] Interestingly, various types of proteins, such as hormones, neurotransmitters, and digestive enzymes, are likewise transported out from cells in secretory vesicles,[12] possibly osmotically inactivated in a way similar to that of histamine. Indeed, charged proteins have been shown to interact with oppositely charged weakly cross-linked synthetic polymers, strongly reducing the swelling of the latter.[15]

The swelling of polyelectrolyte gels is affected also by the absorption of oppositely charged surfactant from solution.[16] Highly charged surfactant micelles replace the network counterions, thereby reducing the swelling pressure in the gels.[17−20] In a bulk solution of surfactant, the gels undergo a volume change from highly swollen to very collapsed, in the latter state containing, typically, only 50 wt % water.[21] The resulting polyion−surfactant complexes are highly ordered on the microscopic scale.[21−24] The basic building blocks can be described as globular or cylinder-shaped "polyion-dressed micelles",[25] packed close together on cubic or hexagonal lattices, respectively. The association of micelles with network chains is favorable compared with the self-assembly in pure surfactant solutions.[25] The major reason for this is that the association is followed by a release of network counterions, whereas in the solution surfactant counterions become bound to the micelles. Thus, in salt-free systems the critical association concentration (cac) is orders of magnitude lower than the cmc. In studies of macroscopic gels (volumes on the order of 1 mL), where bulk conditions are generally not met, the amount of surfactant absorbed is often not sufficient to collapse the entire gel. Interestingly, in this case the surfactant distribution in the gel becomes highly nonuniform. Typically one observes the formation of a dense surface phase ("skin") surrounding a swollen core due to a phase separation between swollen and collapsed regions in the gel.[21,26,27] The skin formation takes place when both preswollen and dry gels are placed in surfactant solutions.[28] The skins have compositions and micelle structures similar to

* To whom correspondence should be addressed. E-mail: Per.Hansson@farmaci.uu.se.

10.1021/jp027583e CCC: $25.00
Published on Web 08/06/2003

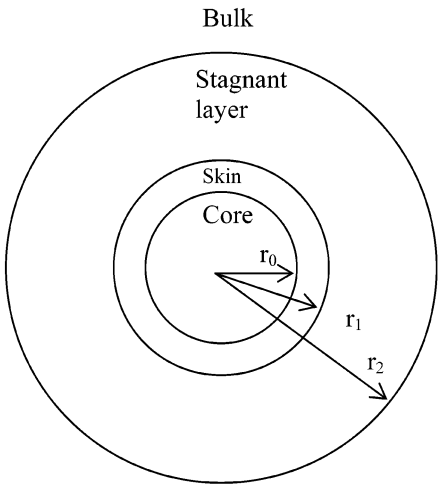

Figure 1. Model of a phase-separated gel surrounded by liquid. A swollen core is surrounded by a collapsed surface phase (skin) and a stagnant liquid layer. The latter is an idealization used to describe the mass transfer between the gel and the bulk liquid.

those of fully collapsed gels. However, as pointed out in a recent paper,[28] the deformation of the skin network is anisotropic. The reason for this is that the swelling of the core leads to a lateral extension of the collapsed surface phase, with a corresponding nonuniform deformation of the polymer network on the microscopic scale. Importantly, due to their rubber-like elasticity, the skins reduce the equilibrium gel swelling by imposing a pressure on the core.[28] Surface phases have been observed also in other types of gels responding to environmental changes, e.g., temperature jumps,[29] but only as transient structures.[30,31] The factors controlling the volume transition are different for different systems; e.g., heat transfer is faster than surfactant mass transfer (diffusion). However, for two phases with different swelling to coexist in the same network, one necessary criterion should be that the extent of swelling of the dominating phase deviates as little as possible from the swelling it would have in the absence of the other phase. Thus, the appearance of the collapsed phase at exterior parts of spherical or globular gels may be explained by the fact that it allows for the largest swelling of the swollen part, i.e., the core.[28,32−35]

As part of our investigation of the mechanisms behind skin formation and the effect of skins on gel swelling, we investigate in the present paper the relation between surfactant self-assembly and gel volume transition in gels of sub-millimeter size. We demonstrate that skins appear as intermediate states when spherical sodium polyacrylate (NaPA) gels collapse in bulk solutions of dodecyltrimethylammonium bromide (DoTAB). Once that has been established, we isolate the most important processes, determining the onset of micelle formation/phase separation and the kinetics of shrinking in such gels. For that purpose we begin the paper by considering theoretically the case of diffusion-controlled surfactant absorption and the coupling to volume changes of core/skin gels. At the end of the paper the theory is compared with the results from time-resolved microscopy studies of gels shrinking in surfactant solutions.

Theory

The model used to describe a phase-separated gel immersed in a bulk liquid medium is schematically represented in Figure 1. The gel consists of a solvent-swollen core of radius r_0 and a surface phase (skin) with outer radius r_1. Outside the gel there is a "stagnant" liquid layer with outer radius r_2. The gel volume is given by[28]

$$V = V_{\text{skin}} + V_{\text{core}} \tag{1a}$$

$$V_{\text{skin}} = n_{\text{p}}\beta' v_{\text{skin}} \tag{1b}$$

$$V_{\text{core}} = n_{\text{p}}(1 - \beta')v_{\text{core}} \tag{1c}$$

where v_{core} and v_{skin} are the volumes of the core and skin, respectively, per mole of polymer units, n_{p} is the number of moles of PA (monomer) units in the gel, and β' is the fraction of them in the skin. For PA gels absorbing CTAB or CTAC, β' was previously[28] found to be equal to β, the average number of absorbed surfactant molecules per PA monomer. This means that the molar ratio of surfactant to polyion in the skins equals unity. We shall assume that to be the case also in the present system. With a volume $V_0 = n_{\text{p}}v_0$ of the surfactant-free gel ($\beta = 0$), one obtains from (1)

$$\frac{V}{V_0} = \frac{v_{\text{core}}}{v_0} - \left(\frac{v_{\text{core}} - v_{\text{skin}}}{v_0}\right)\beta \tag{2}$$

The situation we intend to describe is the network in equilibrium with a bulk aqueous solution of 10 mM NaBr to which, at time zero, a given amount of surfactant is added. The absorption of surfactant leads to a shrinking of the gel. Experiments (see below) indicate that it is meaningful to distinguish between the surfactant absorption prior to and after micelle formation starts in the gel. During the first period, which we shall refer to as the *lag period*, surfactant monomers accumulate in the gel with negligible effects on the gel volume. The second period, characterized by gel *shrinking*, will be assumed to start when cac in the gel is reached. In the present approximate treatment we shall describe separately the absorption of surfactant below and above the cac. Our ansatz is that the rate-controlling step during both processes is diffusion of surfactant from the bulk to the core. It will thus be assumed that the gel has time to maintain swelling equilibrium at all times during surfactant absorption. In the following sections we will establish equations describing the equilibrium swelling and the transport of surfactant into the gel and then combine them to find expressions describing the kinetics of gel shrinking.

Swelling Equilibrium. The skin is permeable to water, surfactant, and simple ions. Swelling equilibrium is thus reached when the osmotic pressure is the same in the core and in the solution. Recently, Hansson et al.[28] described the swelling of core/skin gels. They found that the condition for swelling equilibrium of the core could be written as

$$\Delta\pi_{\text{ion}} + \pi_{\text{net}} + \pi_{\text{skin}} = 0 \tag{3}$$

where $\Delta\pi_{\text{ion}}$ is the swelling pressure due to the difference in ion activity between the core and the solution and π_{net} and π_{skin} are the contributions to the osmotic pressure in the core from the work of deforming the core network and the skin, respectively.

To estimate $\Delta\pi_{\text{ion}}$, we consider the distribution of salt between the solution and core. This can be calculated from the Donnan theory[36] using the counterion condensation theory[37] to correct for ion binding to the polyion. For a 1:1 electrolyte, this leads to the expression (see Appendix 1)

$$\Delta\pi_{\text{ion}} = 2RTC_{\text{salt}}[[(2v_{\text{core}}\xi C_{\text{salt}})^{-2} + 1]^{1/2} - 1] \tag{4}$$

where R is the ideal gas constant, T is the absolute temperature, C_{salt} is the electrolyte concentration in the solution (including

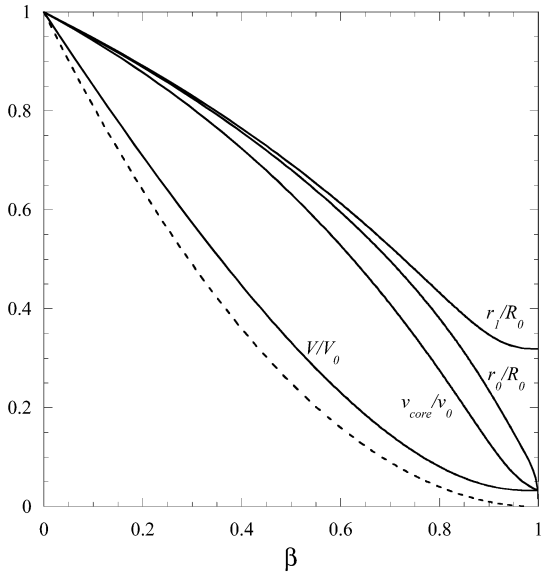

Figure 2. Dependence of relative gel volume (V/V_0), core swelling ($\upsilon_{core}/\upsilon_0$), gel radius ($r_1/R_0$), and core radius ($r_0/R_0$) on the amount of absorbed surfactant per charged group of the network, β, according to the model for equilibrium swelling. Physical parameters used in (2)−(6): $p = 50$, $\upsilon_{skin} = 7 \times 10^{-4}$ m^3/mol, $C_{salt} = 10$ mM, $\xi = 2.85$, $T = 298$ K. Dashed line: $V/V_0 = (1 - \beta)^2$.

the surfactant), and ξ is the dimensionless linear charge density parameter ($\xi = 2.85$ for PA in water at 25 °C; see Appendix 1).

π_{net} can be obtained from the data of 1% cross-linked PA gels swelling in surfactant-free sodium chloride solutions, as described elsewhere.[28] With $\Delta\pi_{ion}$ calculated from (4) the following result is obtained from a fit to the data reported by Hansson et al.:[28]

$$\pi_{net} = -1.05 \times 10^4 - 1.46 \times 10^5 \upsilon_{core} \qquad (5)$$

where the pressure is obtained in units of Pa when υ_{core} is expressed in units of m^3/mol. Note that the sum of $\Delta\pi_{ion}$ and π_{net} describes the swelling of the pure network at different osmotic pressures in the solution. Therefore, systematic errors in the description of $\Delta\pi_{ion}$ are largely canceled by identical errors in π_{net}.

When the volume of the surface phase is constant, π_{skin} can be calculated from the theory of rubber elasticity due to Wall.[38] For the present purpose the result is conveniently expressed as a function of υ_{core}:

$$\pi_{skin} = -\frac{\beta}{1-\beta}\frac{2RT}{3p\upsilon_{skin}^{2/3}\upsilon_{core}^{1/3}}\left(1 - \left(\frac{\upsilon_{skin}}{\upsilon_{core}}\right)^2\right) \qquad (6)$$

where p is the average number of monomer units between two cross-links in the network. For a derivation of (6) and a test of its applicability to NaPA gels, see the paper by Hansson et al.[28] In Figure 2 we have calculated, using the above model, the equilibrium swelling (V/V_0) as a function of β; values of input parameters used are given in the figure legend. Shown are also theoretical estimates of $\upsilon_{core}/\upsilon_0$, r_0/R_0, and r_1/R_0 obtained with the same parameters, and the function $V/V_0 = (1 - \beta)^2$ (see below). R_0 is the gel radius prior to shrinking.

Lag Period. At time zero, the surfactant concentration in the bulk is uniform but there is no surfactant inside r_2. During the lag period surfactant monomers enter the stagnant layer and the core to mix with sodium ions. No skin forms; thus, $r_0 = r_1$ and V is constant. Even under such conditions a description of the ion exchange is complex due to electric coupling of the ionic fluxes. In the present analysis we shall assume that sodium and surfactant ions have equal mobility. This means that the exchange is governed by a single diffusion coefficient. The approximation is good when one of the ions is in large excess, which is the situation considered here. In this case the diffusion rate of the minority component (here $DoTA^+$) is rate controlling.[39] Furthermore, it will be assumed that the net concentration of positive and negative ions is unchanged everywhere in the system and that the diffusion through the stagnant layer is the rate-determining step. This situation has been thoroughly examined in the literature of ion-exchange resins.[39] The assumption of stagnant layer control is consistent with a uniform concentration of ions in the gel at all times during the lag period. Due to chemical differences the partitioning of sodium ions and surfactant between the gel and the liquid phase at r_0 is given by[39]

$$\frac{C_{s,g}}{C_{Na,g}} = \alpha\frac{C_{s,0}}{C_{Na,0}} \qquad (7)$$

where $C_{s,g}$ and $C_{Na,g}$ are the concentrations of surfactant and sodium ions in the gel, respectively, $C_{s,0}$ and $C_{Na,0}$ are the corresponding concentrations at r_0, and α is a selectivity coefficient (see below).

At steady state the rate of transport of surfactant into a spherical gel is[40]

$$\frac{dn_{s,g}}{dt} = \frac{4\pi r_0 r_2 D_{II}(C_{s,2} - C_{s,0})}{r_2 - r_0} \qquad (8)$$

where $n_{s,g}$ is the number of moles of surfactant in the gel and D_{II} is the effective diffusion coefficient in the stagnant layer. In the present case where $C_{s,2}$ is constant the solution to the differential equation (8) can be written as[39]

$$t_U = \frac{r_0^2(1 - r_0/r_2)C_g}{3D_{II}\alpha C_{salt}}\{(\alpha - 1)U - \ln(1 - U)\} \qquad (9)$$

where t_U is the time for fractional attainment of equilibrium $U(t)$ and C_g is the total concentration of positive ions in the gel. $U(t)$ is defined by

$$U(t) = \frac{C_{s,g}(t)}{C_{s,g}(\infty)} = \frac{C_{s,g}(t)}{\alpha C_g}\left(\frac{C_{salt}}{C_{s,2}} + 1 - \alpha\right) \qquad (10)$$

where $C_{s,g}(t)$ is the average concentration of surfactant in the gel at time t and $C_{s,g}(\infty)$ is the concentration at equilibrium if no micelles would form. The last equality in (10) follows from (7), taking into account that, at equilibrium, and in the absence of skin, $C_{s,0} = C_{s,2}$. The time t_{cac} required to reach cac in the gel (cac_g) is obtained by putting $C_{s,g}(t) = cac_g$ in (10) and substituting for $U(t)$ in (9). To obtain the total lag time t_L, one should add to t_{cac} the time to reach steady-state flow in the stagnant layer, which is approximately equal to $(r_2 - r_0)^2/2D_{II}$:

$$t_L \approx t_{cac} + (r_2 - r_0)^2/2D_{II} \qquad (11)$$

Kinetics of Gel Shrinking. Micelles form when the surfactant concentration in the gel is equal to cac_g. At that point, and under conditions of stagnant layer control, the concentration in the gel is related to that outside by

$$\frac{\mathrm{cac_g}}{C_\mathrm{g} - \mathrm{cac_g}} = \alpha\frac{C_{\mathrm{s},0}(t_\mathrm{L})}{C_\mathrm{salt} - C_{\mathrm{s},0}(t_\mathrm{L})} = \alpha\frac{\mathrm{cac}}{C_\mathrm{salt} - \mathrm{cac}} \quad (12)$$

The last equality follows since $C_{s,0}(t_L) = C_{s,1}(t_L) = \mathrm{cac}$, where cac is the surfactant concentration in the bulk—at equilibrium—when the concentration in the gel is equal to $\mathrm{cac_g}$. Previous studies[27,28] of equilibrated gels indicate that phase separation takes place immediately above $\mathrm{cac_g}$. By assuming that skin formation starts at $\mathrm{cac_g}$, the concentration of surfactant in the core will be equal to $\mathrm{cac_g}$ when $t \geq t_L$ (see below). This follows from the assumption that the transport of surfactant to the core is the rate-determining process. However, if the skin presents a diffusion barrier, the surfactant concentration just outside the gel ($C_{s,1}$) will be larger than cac. We do not know the mechanism of transport in the skin. Nevertheless, at steady state, the difference in chemical potential across the skin will correspond to a concentration difference equal to $C_{s,1} - \mathrm{cac}$. Note that cac is the activity of surfactant monomers in quasi-equilibrium with the core (related to $\mathrm{cac_g}$ by a Donnan potential). To obtain the correct form of Fick's law, we must use instead of the diffusion coefficient in the skin (D_I) the permeability, P:

$$\frac{\mathrm{d}\beta}{\mathrm{d}t} = \frac{1}{n_\mathrm{p}}\frac{\mathrm{d}n_{\mathrm{s,g}}}{\mathrm{d}t} = \frac{v_0}{V_0}\frac{\mathrm{d}n_{\mathrm{s,g}}}{\mathrm{d}t} = \frac{v_0}{V_0}\frac{4\pi r_0 r_1 P}{r_1 - r_0}(C_{\mathrm{s},1} - \mathrm{cac}) \quad (13)$$

In (13) we have assumed that surfactant molecules entering the core instantly form micelles and hence become classified as bound. By assuming steady-state conditions, i.e., that the flow is equal at all $r \geq r_0$, we can eliminate $C_{s,1}$ and relate, instead, the binding rate to the bulk surfactant concentration $C_{s,2}$:

$$\frac{\mathrm{d}\beta}{\mathrm{d}t} = \frac{v_0}{V_0}\left(\frac{4\pi r_1 r_2 D_\mathrm{II}(C_{\mathrm{s},2} - \mathrm{cac})}{r_2 - r_1 + (D_\mathrm{II}/P)(r_1 - r_0)r_2/r_0}\right) \quad (14)$$

The derivation of (14) is outlined in Appendix 2. By integrating (14) from $t = t_L$ ($\beta \approx 0$) to $t = t' + t_L$ ($\beta = \beta_{t'}$), we obtain

$$t' = \frac{{R_0}^3}{3v_0 D_\mathrm{II}(C_{\mathrm{s},2} - \mathrm{cac})}\int_0^{\beta_{t'}}\left(\frac{1}{r_1} - \frac{1}{r_2} + \left\{\frac{1}{r_0} - \frac{1}{r_1}\right\}\frac{D_\mathrm{II}}{P}\right)\mathrm{d}\beta \quad (15)$$

where R_0 is the radius of the gel prior to shrinking and r_0 and r_1 are functions of β; see (1):

$$r_0 = R_0[(1 - \beta)v_\mathrm{core}/v_0]^{1/3} \quad (16a)$$

$$r_1 = R_0[(1 - \beta)v_\mathrm{core}/v_0 + \beta v_\mathrm{skin}/v_0]^{1/3} \quad (16b)$$

Note that $t' = t - t_L = 0$ when the shrinking starts. The relation between r_2 and r_1 will be dealt with in the next section. Since the core is assumed to be in quasi-equilibrium at all times, (3)−(6) provide the relationship between v_core and β needed to evaluate the integral in (15). The integration must be made numerically. The result can be used in (2) to obtain the gel volume as a function of time. For an approximate closed form expression, see Appendix 3.

Stagnant Layer Thickness. The stagnant layer thickness d ($= r_2 - r_1$) is a fictitious quantity and cannot be measured directly. However, in the literature on mass transfer it is defined as the ratio between D_II and the mass transfer coefficient.[41] Its magnitude can be calculated from dimensionless numbers. For single spherical particles[41]

$$d = \frac{2r}{Sh} \quad (17)$$

where Sh is the Sherwood number and r is the particle radius. When the bulk liquid flow is zero, $Sh = 2$, so $d = r$. In this case the assumption of a stagnant layer gives the same result as the exact solution of the diffusion equation for steady-state radial diffusion in an unstirred infinite bulk. For conditions of forced convection Sh is a function of the Reynolds (Re) and Schmidt (Sc) numbers:[41]

$$Sh \approx 2.0 + 0.6(Re)^{1/2}(Sc)^{1/3}\ (Re < 20) \quad (18a)$$

$$Re = \frac{2vr\rho}{\eta} \quad (18b)$$

$$Sc = \frac{\eta}{\rho D} \quad (18c)$$

where v is the flow rate in the liquid, ρ is the particle density, η is the liquid viscosity, and D is the diffusion coefficient. Since $d = r_2 - r_1$, (17) gives $r_2 = (2/Sh + 1)r_1$, and $r_1 r_2/(r_2 - r_1) = (Sh/2 + 1)r_1$. At a given flow rate in the liquid, these equalities can be used to eliminate r_2 in (15).

Experimental Section

Materials. DoTAB (99%+) from Serva, pyrene (analytic grade) and acrylic acid from Aldrich, sodium bromide (NaBr) from Bakers, sodium chloride (NaCl), sodium hydroxide (NaOH), and paraffin oil (for spectroscopy) from Merck, and *N*,*N*,*N*′,*N*′-tetramethylenediamine (TEMED) (99%+), *N*,*N*′-methylenebisacrylamide, and ammonium persulfate from Sigma were used as received. All solutions were prepared with high-quality Millipore water.

Preparation of Gels. Sub-millimeter gel beads were prepared by inverse suspension polymerization using paraffin oil as the continuous phase. A solution of acrylic acid (1.4 M), 12 mM *N*,*N*′-methylenebisacrylamide (cross-linking agent), and 5 mM TEMED (accelerator) was prepared. The acrylic acid was converted to acrylate by the addition of sodium hydroxide (to 2 M) to prevent it from partitioning into the oil. Sodium chloride (2.6 M) was added to screen the charges of the reactants. A 1 mL sample of the reaction mixture was mixed with 10 μL of a 0.18 M ammonium persulfate solution (radical initiator) and injected into the preheated, heavily stirred oil. The reaction mixture was dispersed into sub-millimeter droplets by mechanical agitation using a magnetic stirrer. Gelation took place almost immediately. The reaction was carried out in a nitrogen atmosphere to prevent quenching by oxygen. The reaction mixture was degassed prior to injection. The oil was degassed and heated in the reaction vessel to 100 °C for 1 h, before it was cooled to the reaction temperature (60 °C). The reaction was quenched after 1 h by injection of water into the suspension, and gel beads were transferred from the reaction vessel to a vial. The oil−gel slurry was mixed with saturated sodium chloride solution and centrifuged. The top phases (containing paraffin oil and excess aqueous phase) were discarded and the gel beads transferred to a beaker and repeatedly washed alternating with 0.1 M sodium chloride and acetone to remove any unpolymerized material and oil residues. Finally the gels were equilibrated with large amounts of Milli-Q water.

Sieving. Inverse suspension polymerization creates a broad size distribution, making sieving necessary to produce samples

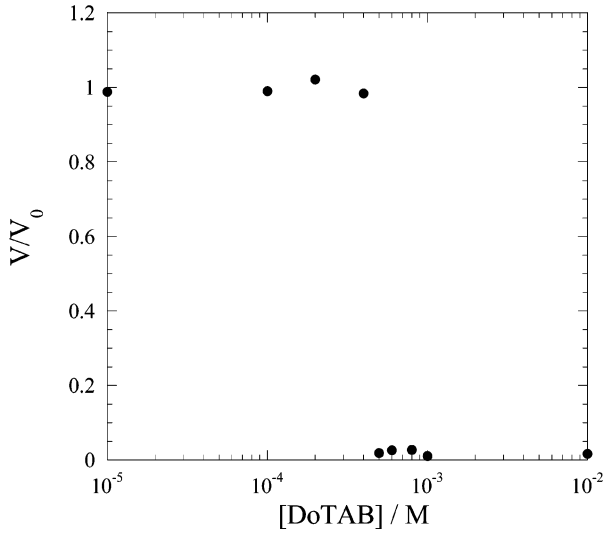

Figure 3. Equilibrium swelling of NaPA gels ($R_0 = 55-80$ μm) in solutions of DoTAB and 10 mM NaBr. The relative volume (V/V_0) is plotted vs bulk surfactant concentration (logarithmic scale).

suited for microscopy. Fractions between 100−160 and 160−315 μm were collected by hand sieving using sieves from Retsch.

Light Microscopy. Single gel beads were monitored using a light microscope (Karl Zeiss Axioplan 2) equipped with a digital camera (Cohu CCD High Performance). In all experiments (except where stated otherwise) the gels were in contact with a bulk solution of the surfactant containing 10 mM NaBr and small amounts of NaOH (the latter was present to keep the network fully charged; pH > 9). To accomplish bulk conditions, the experiments were carried out in the following way. A microscopy slide was positioned on a frame inside beaker. The beaker was filled with surfactant-free solution, and gel beads were placed on the slide using a pipet so that they were positioned just below the air/solution interface. At time zero 0.10 mL of a DoTAB stock solution was carefully injected into the solution close to the bottom of the beaker. Mixing was accomplished by pumping parts of the solution in and out a couple of times using a Pasteur pipet. The final DoTAB concentrations were 0.1, 1, 2, 4, 5, 6, 8, 10, and 100×10^{-4} M. Pictures were taken (Zeiss microscope) on a gel bead at fixed time intervals until no volume change could be observed. Images were analyzed with Easy Images analyzing software from Bergströms Instruments. Each image was evaluated separately, and the projected particle area was measured. Gel bead diameters and volumes were calculated by assuming the beads were spherical. Separate studies of wrinkling gels were made using an Olympus BX51 microscope.

Fluorescence Microscopy. In separate experiments the distribution of surfactant micelles in individual gels was monitored using an Olympus BX51 fluorescence microscope. Gel beads were placed in a solution containing 10 mM NaBr and 0.1 mM NaOH. A mixture of DoTAB and pyrene was injected into the bulk to total concentrations of 1 mM and 1 μM, respectively.

Results and Discussion

Equilibrium Swelling. The volumes of gels equilibrated in DoTAB solutions were determined as described in the Experimental Section. Figure 3 shows the relative volume (V/V_0) at equilibrium as a function of surfactant concentration. V_0 is the gel volume in 10 mM NaBr (pH $\approx$ 9) in the absence of surfactant. At low DoTAB concentrations the gels remain in the swollen state, independent of surfactant concentration. Note, since surfactant monomers are greatly outnumbered by NaBr, their contribution to the osmotic pressure is negligible at this stage. At DoTAB concentrations larger than ca. 0.5 mM the gels are in a collapsed state. No reswelling is observed at higher surfactant concentrations (studied range 0−10 mM). All surfactant concentrations used were below the cmc of the surfactant (cmc = 11 mM in 10 mM NaBr[42]).

Relation between cac and Gel Collapse. The transition between swollen and collapsed states takes place in a narrow range of DoTAB concentrations. It was found in a previous study[18] of PA/DoTAB slab gels (centimeter-sized) that the volume transition was due to the formation of micelles in the gels. In particular, the concentration of surfactant inside gels at which micelles could be detected was close to the cac in an equally concentrated solution of linear NaPA. In that study the amount of surfactant inside the gels was determined from the measured depletion of surfactant in the solution in equilibrium with slab gels. Such measurements are not possible in the present case. However, to be able to compare with experiments on slab gels, we shall make a rough estimate by calculating from the Donnan theory and the bulk surfactant concentration the amount of surfactant in gels at the onset of gel collapse. From swelling experiments reported earlier, $C_{p,g}$ ($=1/v_{core}$) is estimated to be 45 mM for NaPA gels with the present degree of cross-linking, a factor of 2.2 larger than in pure water. (The same result is obtained by inserting (4) and (5) and $\pi_{skin} = 0$ into (3), and solving for v_{core}.) From this and with $\xi = 2.85$ and $C_{salt} = 10$ mM, (A:1) and (A:2) give $C_{+,g} = 21$ mM and $C_{-,g} = 4.8$ mM. Thus, the total concentration of positive ions in the gel is 50 mM (the polyion counterions plus those entering from the solution). Just prior to the volume transition the bulk concentration ratio of $DoTA^+$ over Na^+ is 0.04 ($=C_{s,0}/C_{Na,0}$). If the ion distribution were entirely statistical, this would also be the ratio in the gel. However, the polyacrylate network has a preference for Na^+ over $DoTA^+$, as was shown in an earlier study,[18] where the selectivity coefficient (α) was determined as 0.2. (Note that the selection by polyion networks of one counterion in preference to the other is expected and well-known to the literature of ion exchangers.[39]) With $\alpha = 0.2$ and with $C_{Na,g} + C_{s,g} = 50$ mM, we obtain from (7) $C_{s,g} = 0.4$ mM. This value is in perfect agreement with cac_g determined for the surfactant in equally swollen NaPA slab gels, suggesting that micelle formation is equally favorable in both systems.

It is worth noting that the gel volume transition takes place at a bulk DoTAB concentration close to cac for the surfactant in 10 mM NaBr/Cl solutions of linear NaPA, reported earlier.[43,44] (The fact that this concentration is also equal to cac_g is just a coincidence.) To appreciate the significance of this observation, it is necessary to recall the most important factors determining the cac. A thermodynamic analysis of micelle formation in polyelectrolyte systems shows that the following equation is applicable to DoTAB in dilute NaPA solutions:[25]

$$k_B T \ln(\text{cac}) = \Delta\mu^\circ + 2\gamma a - \mu_{p,el} \qquad (19)$$

where $\Delta\mu^\circ$ is the standard free energy change of taking the surfactant hydrocarbon tail from water to the micelle core, a is the optimal area per surfactant in the micelle headgroup region, γ is a "surface tension", and $\mu_{p,el}$ is the electrostatic free energy of the polyelectrolyte solution per polyion charged group. For a given aggregation number (N) the first two terms can be treated as constants. Experiments show[25,45] that N for $DoTA^+$ depends

on the properties of the polyion, but is essentially independent of salt and polyelectrolyte concentrations in a wide range of concentrations. However, $\mu_{p,el}$ is very sensitive to such environmental changes, meaning that cac is strongly dependent on the concentration of electrolyte. It is a familiar result from polyelectrolyte theory[46] that the electrostatic energy of a highly charged polyion is considerably lowered by the binding of counterions, but little dependent on salt and polyelectrolyte concentrations. (Thus, the sensitivity of $\mu_{p,el}$ to the electrolyte concentration is mainly a counterion entropy effect.) According to the counterion condensation theory[37] (see above), the effective charge of a polyion is renormalized in such a way that each charged group is associated with $1 - \xi^{-1}$ "condensed" counterions. In an excess of salt we can write for a given type of polyion

$$\mu_{p,el} \approx \text{constant} - (1 - \xi^{-1})k_B T \ln C_{salt} \qquad (20)$$

(20) is valid as long as the polyion chains are in equilibrium with a bulk salt solution, as is indeed the case for the gels studied here. Hence, given C_{salt} and the type of polyion (referring to the constituents of the backbone), one expects from (19) and (20) polyion-dressed micelles to appear at about the same bulk DoTAB concentration in the cross-linked and the linear cases. This is in agreement with what we observe here.

In centimeter-sized PA gels, the swelling was found[18,27,28] to be controlled by the amount of surfactant absorbed by the gels, which was easily adjusted as the gels took up essentially all surfactant that was added to the solutions. Gels with $\beta > 0.8$ were in a collapsed state. Further absorption led to no significant volume changes (within the studied range of compositions). Importantly, however, all gels with intermediate surfactant loading contained two macroscopic phases: a micelle-free swollen core and a dense micelle-rich surface phase (skin). The swelling of such gels is intermediate between those of fully swollen and collapsed gels, and is well accounted for by the theory in (2)−(6).[28] Apparently the phase separation started just above cac_g (a study of the properties of the surface phase very close to cac_g in PA/DoTAB gels is presently being undertaken). The behavior is analogous to that of linear PA/DoTAB mixtures,[47] which can be attributed to a net attraction between polyion-dressed micelles (see ref 25 for details). Phase studies of the latter system show[47] that the gap between cac and the phase boundary is very small for PA concentrations similar to those in the present gels. In principle, phase separation in the case of a linear polyion would correspond to a discrete volume transition at a given bulk surfactant concentration (just above cac) in the cross-linked system, at least for gels in contact with a solution containing an excess of simple salt. (At low salt concentrations and a finite solution volume a gradual transition takes place, as shown elsewhere.[18]) However, due to long-range interactions in gels the critical surfactant concentration for collapse may be somewhat higher than the phase transition concentration in the linear system.[33] Furthermore, from a comparison with temperature-sensitive gels, where the transition temperature has been found[30] to be different for collapse and swelling transitions, the critical surfactant concentration for swelling of collapsed gels is expected to be lower than the collapse concentration (hysteresis). Temperature-induced transitions have been analyzed theoretically.[33,35] For transitions of the type observed in the present paper, where two phases coexist in the gel, there is a coexistence cost in elastic free energy of deformation.[34] Therefore, to overcome the coexistence cost, the transition temperature must be higher (or lower) than the Maxwell temperature, i.e., the transition temperature when the two phases do not have to coexist in the same gel.[35] With the same argument taken over to the present system, and the transition temperature replaced by the critical collapse concentration of surfactant, a discrete volume transition is expected since the elastic free energy of the network decreases as the gel collapses.

We conclude from this section that sub-millimeter gels in a bulk surfactant solution display a sharp volume collapse at conditions where polyion-dressed micelles are expected to be formed on the basis of the knowledge of the behavior of linear polyions in solution and cross-linked centimeter-sized gels. It is not possible from the present set of data to conclude that there is a true discontinuity (first-order transition) in the volume transition curve. It should be mentioned, however, that Sasaki et al.[48] recently found that thin cylinder-shaped NaPA gels (ca. 0.7 mm in diameter) displayed an apparently discrete volume transition in solutions of dodecylpyridinium chloride containing an excess of NaCl. In the following sections we study dynamic aspects of the transition of gels from the fully swollen to the collapsed state at surfactant concentrations above cac.

Phase Coexistence during Volume Transition. Microscopy images showing the time evolution of gels during shrinking are presented in Figure 4. Two main categories of behavior were observed. In Figure 4a, the gel maintains essentially its original shape and the surface is smooth. In Figure 4b, shrinking is accompanied by patterning of the gel surface during later stages of the collapse. Since the formation of micelle-rich skins was proved by fluorescence microscopy (see below), we interpret the patterns as wrinkling of skins. The gel shown in Figure 4b is captured during late stages of the volume transition ($V/V_0 \leq 0.4$). In this particular case a displacement of the skin to one side of the gel took place, resulting in a very asymmetric shape, probably influenced by the adherence of the gel to the microscopy slide. No systematic studies were made, but wrinkling and surface patterns seemed to appear more frequently for large gels and at surfactant concentrations close to the cac. Sasaki and co-workers[19,48] have reported surface patterns for cylinder-shaped NaPA gels interacting with dodecylpyridinium chloride. Patterning appears to be a general feature of polymer gels undergoing phase transition.[49] (See also a paper by Cerda et al.[50])

The skins are very thin during the major part of the volume transition and cannot be observed directly in the light microscope. However, the presence of skins comparable in thickness to the wavelength of light was evidenced by colors at the gel surface. As the thickness increased the color changed from blue to red and eventually disappeared. During late stages of the shrinking a skin of uniform thickness could be observed directly in the light microscope, as exemplified by Figure 5 (top) showing a collapsed gel without wrinkles. The distribution of micelles was monitored with fluorescence microscopy using pyrene as the probe dissolved in the micelles. As evident from the fluorescence image in Figure 5 (bottom) the micelles are located in the skin. Swollen parts are essentially free from micelles. Shown in the middle is an image where visible light and fluorescence were monitored simultaneously.

Interestingly, the gel in Figure 5 was captured in a very late stage of the collapse, where we expected the core to be completely consumed. An indication of the same behavior in PA/CTAB macrogels was reported earlier,[28] but was never proved directly. Note that, for the gel in Figure 5, a core radius considerably larger than the skin thickness should not be mistaken for a small amount of absorbed surfactant. As evident from Figure 2, showing theoretical estimates of r_0 and r_1, the

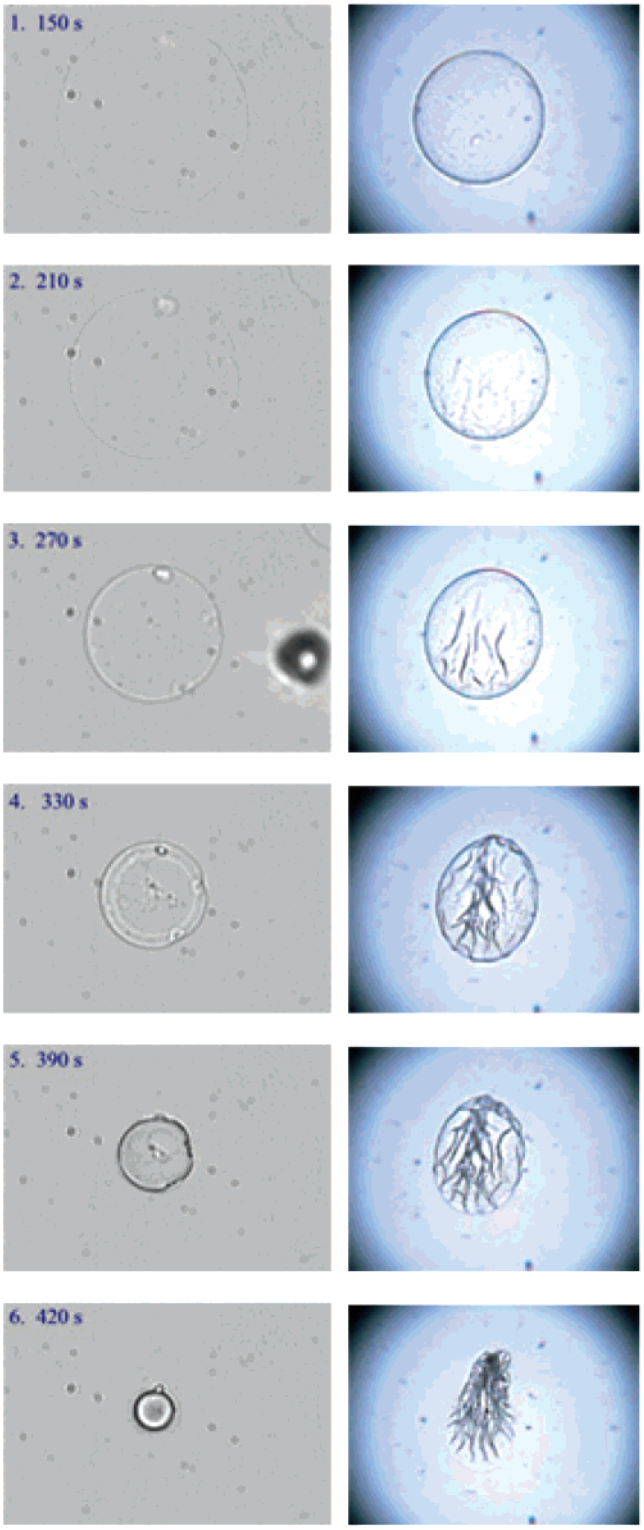

Figure 4. Pictures of NaPA gels taken at different times (indicated) after the addition of 1.0 mM DoTAB to the solution ([NaBr] = 10 mM): (a, left) $R_0 = 57\ \mu$m, (b, right) $R_0 = 280\ \mu$m.

skin thickness is expected to be much smaller than the core radius even at high β. At equilibrium, a skin thickness as for the gel in Figure 5 would correspond to $\beta = 0.8$. Interestingly, in this binding range the core network should be very compressed by the action of the skin (see the ratio v_{core}/v_0 in Figure 2), so the volume is not expected to decrease much upon further binding.[28] However, the cooperativity of the surfactant binding to slab gels has been shown to be small for $\beta > 0.8$; i.e., large surfactant concentrations are needed to convert the last 20% of

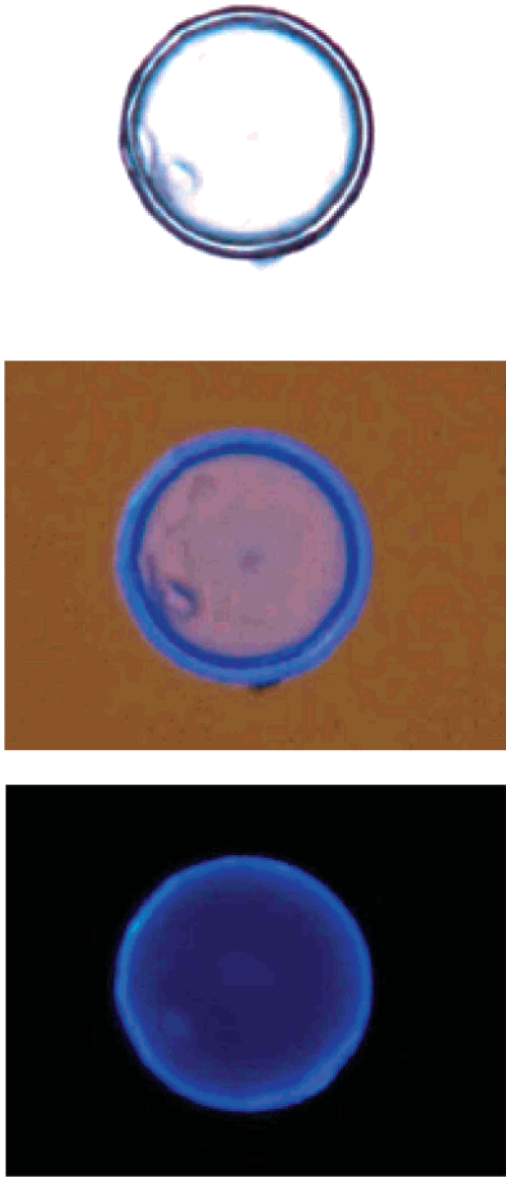

Figure 5. Light microscopy image (top) and fluorescence microscopy image (bottom) of a gel with uniform skin taken 24 h after 0.6 mM DoTAB was added. [NaBr] = 10 mM. In the middle is shown the same gel monitored simultaneously by light and fluorescence microscopy.

the core to skin, if it ever occurs (redissolution of the complexes is a competing process at high concentrations). As already mentioned, no binding data are available for the present microgels. However, if they behave as macrogels with respect to surfactant binding, it is likely that core/shell structures of the type in Figure 5 exist at equilibrium for a range of bulk surfactant concentrations. The observation that the gel shown in Figure 5 remained unchanged after 24 h supports this. A full explanation is presently not at hand, but it may involve the configuration entropy of the polymer chains. The number of states available for the chains in a highly swollen network is small compared with that in the relaxed (collapsed) state. (Remember that the skins behave as perfect rubber; for a discussion, see ref 28.) Therefore, as long as the network is more swollen in the core than in the skin, the complexation between network chains and micelles should increase the polymer configurational entropy. Thus, if this is correct, one motive for surfactant binding to the skin is removed when the core and the skin are equally swollen.

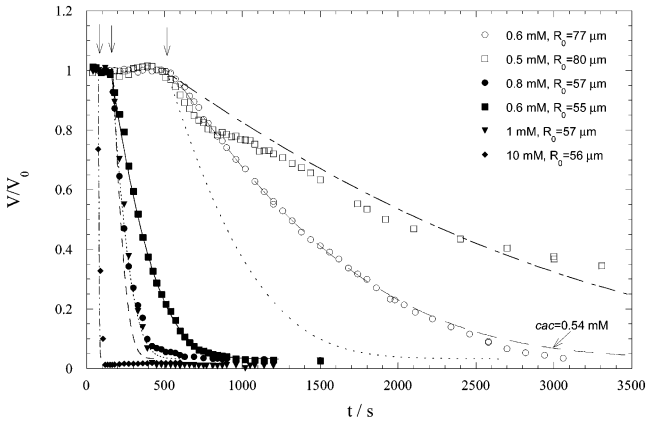

Figure 6. Relative gel volumes (V/V_0) as a function of time after the addition of DoTAB to the solution. Symbols are experimental data for systems with different $C_{s,2}$ and R_0 values (see the legend). Lines are theoretical curves calculated (see the text) with cac = 0.47 mM, $D_{II} = P = 4 \times 10^{-10}$ m^2/s, and $Sh = 2$, except where indicated otherwise. For each curve the system-specific values of $C_{s,2}$ and R_0 were used. Vertical arrows indicate the ends of the three typical lag periods observed.

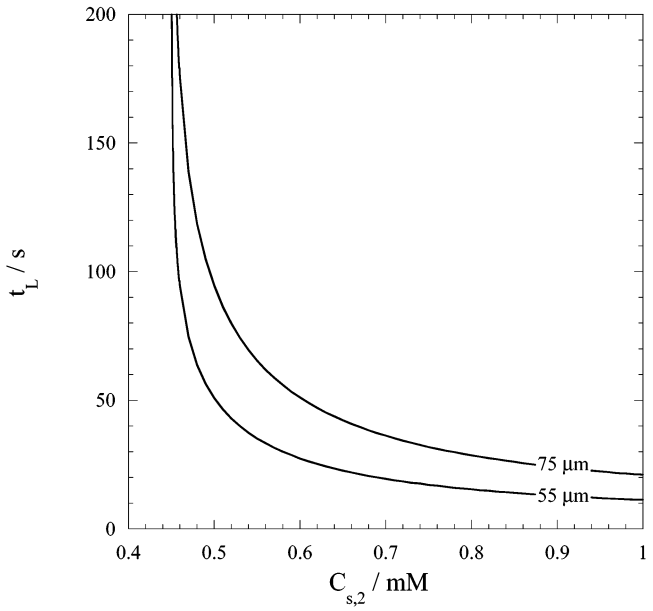

Figure 7. Theoretical lag times (t_L) as a function of bulk surfactant concentration ($C_{s,2}$) for gels with different radii (indicated). The curves were calculated from (9)−(11) with $D_{II} = 4 \times 10^{-10}$ m^2/s,[51] $\alpha = 0.2$,[18] $C_{salt} = 10$ mM, $C_g = 46$ mM, and $r_2 = 2r_0$ ($Sh = 2$).

The existence of surfactant-rich skins in the present gels justifies the model in Figure 1. The result is important as it reveals the presence of surface phases in microgels during the transition from the swollen to collapsed state. Previously, surfactant-induced phase separation has been observed only in centimeter-sized gels. In the following sections we analyze the lag period and the shrinking process, and make comparisons between experiments and model calculations to test the assumption that the transport of surfactant to the core is the rate-determining step.

Kinetics of Volume Transition. The diameter of gels was measured at different times after surfactant was added to the solution ($C_{s,2}$ > cac). The result is shown in Figure 6, where the calculated volume ratio V/V_0 is plotted against time. Note the substantial time delay between the introduction of surfactant and the onset of collapse. In fact, the curves can be divided into two regimes for all gels measured. The first part is the time between surfactant injection and the start of shrinking. During this period essentially no volume or shape changes take place. The second part, the collapse regime, is where the actual volume change occurs. As can be seen in Figure 6 both the length of the lag period and the rate of shrinking strongly depend on the surfactant concentration and the initial size of the gels.

Lag Period. We have seen in previous sections that the volume transition is a consequence of the formation of micelles in the gels. As long as diffusion through the stagnant layer is the rate-determining step, the onset of shrinking should start when the average concentration of surfactant in the gel exceeds cac_g. Our main concern here is to investigate whether the lag times observed can be explained by the diffusive transport of surfactant from the bulk solution to the gels as described by (9)−(11). In Figure 7 we have used these equations to calculate the time to reach a concentration of 0.4 mM $DoTA^+$ in the gels ($\sim cac_g$). The two curves shown were obtained with r_0 equal to 55 and 75 μm, respectively, as were the two typical gel sizes studied. The other input parameters were $D_{II} = 4 \times 10^{-10}$ m^2/s (NMR self-diffusion[51]), $\alpha = 0.2$,[18] $C_{salt} = 10$ mM, and $C_g = 46$ mM. The value of D_{II} is the surfactant self-diffusion coefficient in water, and α was obtained earlier.[18]

The stagnant layer thickness depends on the flow rate in the liquid. In the present experiments there was no stirring after the initial mixing. The convective flow in the liquid was therefore small, so we put $r_2 = 2r_0$ ($Sh = 2$). The theoretical lag times are markedly prolonged close to the cac. This is because the difference in surfactant chemical potential between the bulk and the gel is very small when the concentration in the solution equals cac and the concentration in the gel is just below cac_g.

A comparison shows that the experimental time lags (indicated by arrows in Figure 6) are substantially longer than predicted by theory (Figure 7). Close to cac the theoretical estimates are very sensitive to the choice of input parameters, and it is possible to obtain agreement with experiments by adjusting, e.g., cac_g or α within reasonable limits. However, this does not improve much the agreement at higher surfactant concentrations. There may be several reasons for the poor agreement. One obvious problem is that the theory considers gels surrounded by liquid in all directions, whereas in the experiments they are positioned on a microscopy slide. The flow velocity profile and the surfactant flux in different directions outside a gel are difficult to analyze, but it is likely that the presence of the flat surface slows the influx of surfactant to the gels. However, this is expected to increase the lag time approximately by a factor of 2. Thus, the unexpectedly long lag times observed, in particular at 10 mM DoTAB, call for explanations not based solely on mass transport of ions. The formation of the collapsed phase is a *cooperative* process, with long-range interactions mediated by the elastic network, possibly involving network chains in a surface layer surrounding the entire gel. It could be that the "nucleation" of the surface phase is associated with an energy barrier, so that the swollen state is kinetically stabilized.

Collapse Regime. The lines in Figure 6 represent the results from calculations using the model derived in the theoretical part. All theoretical curves have been adjusted horizontally to begin (at $t' = 0$) where the experimentally observed lag periods end (arrows). As input parameters in the calculations we used for the initial gel radius (R_0), the bulk surfactant concentration ($C_{s,2}$), and the bulk electrolyte concentration ($C_{salt} = 10$ mM + $C_{s,2}$) the appropriate values for each system (see the caption to Figure 6). All other parameters were the same for all systems: cac =

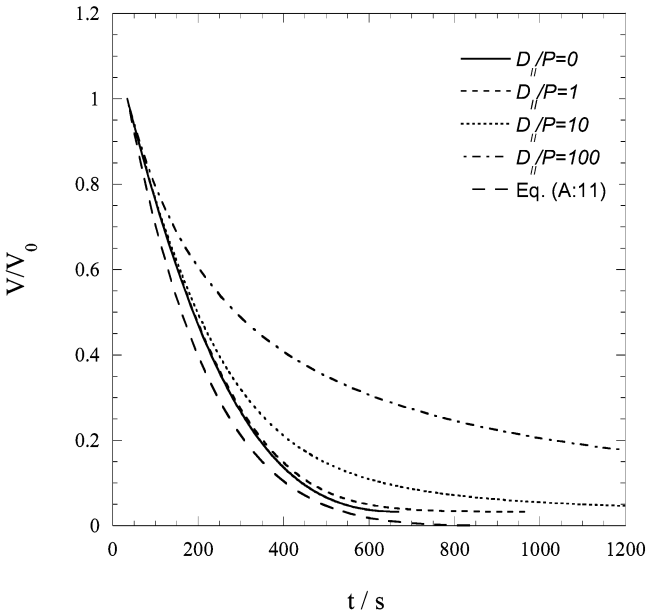

Figure 8. Influence of skin permeability (P) on shrinking kinetics. The theoretical curves were calculated (see the text) with $R_0 = 55\ \mu$m, cac = 0.47 mM, $D_{II} = 4 \times 10^{-10}$ m^2/s, $Sh = 2$, and different values of P (see the legend). Also shown is the result obtained from (A:11) with the same parameters.

0.47 mM, $D_{II} = P = 4 \times 10^{-10}$ m^2/s, and $Sh = 2$. Cac was chosen to give a good fit to the experimental data for 55 μm gels in 0.6 mM DoTAB. Note that this value is in agreement with the critical concentration for volume transition in Figure 3. It can be seen in Figure 6 that with common parameters a fairly good agreement between experiments and theory is obtained, except for the gel with $R_0 = 75\ \mu$m in 0.6 mM DoTAB. In that case a good agreement is obtained with cac = 0.54 mM (see Figure 6), all other parameters unchanged. Of course, the decay rate of the calculated curve depends, essentially, on a product of several parameters; cf. (A:11). Thus, we could have adjusted any of these with a similar result. However, it is clear that, when the bulk concentration is close to cac, even small variations of $C_{s,2}$ or cac have large effects on the shrinking rate. Before this section is closed, it should be pointed out that there could be a flow of liquid from the core to the bulk due to the pressure gradient across the skin during shrinking. This would reduce the surfactant influx. Since the core is assumed to be in quasi-equilibrium at every instance, such complications are, of course, neglected in the model.

Skin Permeability. One parameter has been left out of the discussion so far, namely, the skin permeability P. As shown in Figure 8, theoretical curves calculated for different values of the ratio D_{II}/P do not depend critically on P within certain limits. The solid line represents the case of no resistance for transport through the skin; i.e., $D_{II}/P = 0$. The curve nearly overlaps with the one for $D_{II}/P = 1$. A further increase of the ratio has effects on the latter part of the curves. However, as the skins are initially very thin, the initial parts of the curves are dominated by stagnant layer diffusion, even when the skin permeability is very small.

P is equal to the product of a distribution constant K and the surfactant self-diffusion coefficient in the skin D_I; i.e., $P = KD_I$. Note, as we define it, P is independent of the skin thickness. The concentration of surfactant in skins has previously[21,28] been found to be ca. 1.5 M. The equilibrium monomer concentration is ca. 0.5 mM (=cac), so K is approximately equal to 3000. There are no direct estimates of P or D_I available for the skins. However, for the related DoTAC/water system,[52] D was found to be 5×10^{-13} m^2/s for the surfactant in the cubic micellar phase, as measured by NMR self-diffusion.[53] By using this value, and with the above estimate of K, we obtain $P = 1.5 \times 10^{-9}$ m^2/s, thus 3−4 times larger than D_{II}. If this estimate of P is correct, the transport of surfactant is controlled essentially by stagnant layer diffusion, as indeed the shape of the curves in Figure 6 suggests.

Even though there are reasons to believe the skins to contain a cubic micellar structure similar to the one in the DoTAC/water system, the diffusion coefficient may be different. To illuminate this, we shall consider, briefly, two mechanisms of diffusive transport of surfactant through the skins. A third mechanism, due to diffusion of micelles, is expected to be of no importance.

Studies of surfactant binding to polyions show that there is a "saturation" range where complexes, with little change of composition, are in equilibrium with surfactant solutions of different strengths. If the complexes in the present skins behave in that way, the gradient in chemical potential over the skins could manifest itself simply as a *concentration* gradient in the aqueous "channels" connecting the core and the solution. The transport would be obstructed to an extent given approximately by[54] $D/D_0 = (1 + \phi/2)^{-1}$, where ϕ is the volume fraction occupied by the micelles and D_0 is the diffusion coefficient when $\phi = 0$. This means a reduction of the observed self-diffusion by 20% when $\phi = 0.5$ (skins from macroscopic PA/DoTAB gels contain typically 50 wt % water[21]). In the simplest case with $K = 1$ the effect on P would be negligible in the present context. In principle, if the complexes contained an excess of surfactant over polyion, the Donnan effect would exclude surfactant monomers from the skins, so K would be substantially smaller than 1.

More likely, perhaps, local equilibrium between micelles and monomers is quickly established and maintained in such a way that no concentration gradient develops in the skin. The diffusion can then be looked upon as a random walk of monomers between micelles.[55] With a step length δ equal to the average distance between micelles, and a residence time τ of the surfactant in a micelle, the diffusion coefficient can be written as $D = \delta^2/6\tau$. The simplest possible analysis[56] gives $\tau = 55\tau_0/$cac, with cac in units of M. Here τ_0 is on the order of 10^{-9} s for "normal" micelles.[56] With cac = 0.5 mM and $\tau_0 = 10^{-9}$ s, $\tau = 10^{-3}$ s. The distance between micelles in cubic structures of macroscopic NaPA/DoTAB skins was previously[21] found to be about 42 Å, so we obtain $D_I = 3 \times 10^{-14}$ m^2/s. Finally, with $K = 3000$ we obtain $P = 9 \times 10^{-11}$ m^2/s and $D_{II}/P = 5$. According to Figure 8 such an effect would be small.

Before closing this section, we pay attention to the shrinking curve provided by the approximate relationship in (A:11). The curve, shown in Figure 8, was obtained with the same set of parameters as the exact one for $D_{II}/P = 0$ (solid curve). The disagreement is entirely due to the error introduced by the approximation in (A:7) (the description of the transport kinetics is identical in the two cases). Although (A:11) may be fitted to experimental data, with k as an adjustable parameter, we do not recommend such a procedure. The relationship should be useful, however, for quick estimates of collapse times, or as a reasonable approximation when a closed form expression is needed. It is instructive to compare (A:11) with the Hixon−Crowell[57] cube law for the steady-state dissolution rate of a homogeneous solid particle. As discussed earlier,[28] if the swelling of the gel core were unaffected by the skin, we would have $V/V_0 \approx 1 - \beta$ instead of (A:9), and we would recover the

cube law for homogeneous spheres. This is expected as stagnant layer control is assumed in both cases. The sixth power law in (A:11) reflects the "responsiveness" of the gels due to their elasticity.

Conclusions

We have shown that swollen micrometer-sized gels display a volume transition from swollen to collapsed states. The transition takes place within a narrow range of bulk surfactant concentrations close to the cac in the corresponding system of linear polyion. Just prior to collapse the surfactant concentration in the gel is approximately equal to the cac_g reported for centimeter-sized gels of the same type. Thus, the critical conditions for complex formation between micelles and polyion chains appear to be little dependent on the presence of cross-links and the size of the networks. During volume transition two phases coexist in the gels. The dense surfactant-rich surface phase (skin) grows at the expense of the swollen core network. We have found evidence for phase separation even in the collapsed state, possibly representing an equilibrium situation. The absorption of surfactant takes place in two major steps: there is a lag period with no appreciable volume change and a shrinking period. During the lag period surfactant accumulates in the gels. It appears to be longer than the time required for monomer concentration to reach cac_g via a diffusion-controlled transport from the bulk. One interpretation is that the swollen gels are in a metastable state during nucleation of the surface phase. Once shrinking starts, the kinetics appears to be controlled, essentially, by the diffusion of surfactant from the bulk to the gel core. This means that swelling equilibrium is reestablished on a shorter time scale. Thus, for the systems studied here, mass transfer through the stagnant layer is rate controlling. This case should be intermediary between "skin-controlled" kinetics in slab gels,[58] where the skins soon become thicker than stagnant layers, and "reaction-controlled" kinetics expected in more concentrated surfactant solutions and/or at high liquid flow rates. In the latter case the "reaction" between network chains and surfactant, involving the diffusive motion of network chains,[30] surfactant, simple ions, and water during the self-assembly in the gels, is rate controlling. Such mechanisms have been shown to be rate controlling for the swelling kinetics of highly cross-linked microgels interacting with simple ions and charged drugs.[59,60] Interesting, they may also be of importance for the release of secretory vesicle contents from secretory cells.[61] Of course, no such dynamic aspects are considered in the theoretical analysis presented here.

This is the first microscopy study of gels from our laboratory. We have chosen to work with gels large enough to be macroscopic but small enough to respond quickly to environmental changes. A more detailed comparison between theory and experiment than what has been pursued here is not meaningful at the moment due to experimental difficulties; e.g., better control of the liquid flow is required. There is little doubt, however, that the theory captures the gross effects, including the dependencies on gel size and bulk surfactant concentration. In the future we plan to extend the studies to smaller gel particles.

Acknowledgment. This work has been financially supported by the Swedish Science Council. We are indebted to Göran Dahl for skillful technical assistance and Peter Swensson and Bo Medhage (Pharmacia Upjohn, Uppsala) for disposal of their microscope. We are grateful to Mats Almgren for valuable comments on the manuscript.

Appendix 1

For a 1:1 electrolyte the equilibrium distribution between gel and solution is given by

$$C_{+,g}C_{-,g} = {C_{salt}}^2 \qquad \text{(A:1)}$$

where $C_{+,g}$ and $C_{-,s}$ are the free concentrations (or activites) of positive and negative ions in the gel, respectively, and C_{salt} is the concentration of electrolyte in the solution (including the surfactant). According to the counterion condensation theory[37] in its simplest form, the apparent degree of dissociation of the polyelectrolyte is equal to ξ^{-1}, where ξ is equal to $e^2/4\pi\epsilon_0\epsilon_r k_B T b$. Here, e is the elementary charge, ϵ_0 is the permittivity of a vacuum, ϵ_r is the dielectric constant of the solution, k_B is Boltzmann's constant, and b is the distance between adjacent charges on the polyion. The electroneutrality condition can be written as

$$C_{+,g} = C_{-,g} + C_{p,g}/\xi \qquad \text{(A:2)}$$

where $C_{p,g}$ ($=1/v_{core}$) is the concentration of fixed polyion charges (negative) in the gel core. The swelling pressure is

$$\Delta\pi_{ion} = RT(C_{+,g} + C_{-,g} - 2C_{salt}) \qquad \text{(A:3)}$$

By solving the set of equations (A:1) and (A:2) and after insertion into (A:3) one obtains (4).

Appendix 2

At steady state the surfactant flow is equal at all $r \geq r_0$:

$$\left(\frac{dn_s}{dt}\right)_{r_0} = \frac{4\pi r_0 r_1 P}{r_1 - r_0}(C_{s,1} - \text{cac}) = \frac{4\pi r_1 r_2 D_{II}}{r_2 - r_1}(C_{s,2} - C_{s,1}) = \left(\frac{dn_s}{dt}\right)_{r_1} \qquad \text{(A:4)}$$

Solving for $C_{s,1}$ gives

$$C_{s,1} = \frac{\frac{r_2}{r_0}\left(\frac{r_1 - r_0}{r_2 - r_1}\right)D_{II}C_{s,2} + P(\text{cac})}{P + \frac{r_2}{r_0}\left(\frac{r_1 - r_0}{r_2 - r_1}\right)D_{II}} \qquad \text{(A:5)}$$

Insertion of (A:5) into (13) gives, after rearrangement, (14).

Appendix 3

During the major part of the shrinking process the skin of the gels studied here is very thin compared to the stagnant layer thickness. Therefore, unless the permeability of the skin is very low, it should be a good approximation to neglect the influence of the skin on the transport of surfactant to the core. This means that the third term in the integral in (15) can be neglected, so the expression simplifies to

$$t' = \frac{{R_0}^3}{3v_0 D_{II}(C_{s,2} - \text{cac})}\int_0^{\beta_{t'}} \frac{1}{r_1(Sh/2 + 1)}\, d\beta \qquad \text{(A:6)}$$

Note that, unless the bulk flow rate is zero, Sh is a function of r_1 through (18a,b). The integral in (A:6) is still difficult. To find a simple expression, it is necessary to introduce approximations. The equilibrium model derived earlier[28] suggests the following approximation to be made:

$$\frac{v_{\text{core}}}{v_0} \approx 1 - \beta \tag{A:7}$$

Since $v_{\text{skin}} \ll v_0$, it follows from (16a,b) and (2), respectively, that

$$r_0 \approx r_1 \approx R_0(1 - \beta)^{2/3} \tag{A:8}$$

and

$$\frac{V}{V_0} \approx (1 - \beta)^2 \tag{A:9}$$

Inasmuch as (A:7) is valid, (A:8) and (A:9) are good approximations except when $\beta \approx 1$. By making use of these approximations, and neglecting also the dependence of *Sh* on r_1, the integral in (A:6) is easy. The result is

$$(1 - \beta_{t'})^{1/3} = 1 - \frac{v_0}{{R_0}^2} D_{\text{II}}(Sh/2 + 1)(C_{s,2} - \text{cac})t' \tag{A:10}$$

From (A:9) we obtain

$$\frac{V}{V_0} \approx (1 - kt')^6 \tag{A:11a}$$

$$k = \frac{v_0}{{R_0}^2} D_{\text{II}}(Sh/2 + 1)(C_{s,2} - \text{cac}) \tag{A:11b}$$

References and Notes

(1) Katchalsky, A. *Experientia* **1949**, *5*, 319.
(2) Ricka, J.; Tanaka, T. *Macromolecules* **1984**, *17*, 2916.
(3) Tanaka, T.; Fillmore, D.; Sun, S. T.; Nishio, I.; Swislow, G.; Shah, A. *Phys. Rev. Lett* **1980**, *45*, 1636.
(4) Tanaka, T.; Nishio, I.; Sun, S. T.; Ueno-Nishio, S. *Science* **1982**, *218*, 467.
(5) Hill, T. L. *J. Chem. Phys.* **1952**, *20*, 1259.
(6) Hill, T. L. *Discuss. Faraday Soc.* **1953**, *13*, 132.
(7) Tanaka, T. *Phys. Rev. Lett.* **1978**, *40*, 820.
(8) Melnikov, S. M.; Khan, M. O.; Lindman, B.; Jönsson, B. *J. Am. Chem. Soc.* **1999**, *121*, 1130.
(9) Amiya, T.; Tanaka, T. *Macromolecules* **1987**, *20*, 1162.
(10) Uvnäs, B.; Åborg, C.-H. *News Physiol. Sci.* **1989**, *4*, 68.
(11) Nanavati, C.; Fernandez, J. M. *Science* **1993**, *259*, 963.
(12) Rahamimoff, R.; Fernandez, J. M. *Neuron* **1997**, *18*, 17.
(13) Alberts, B.; Johnson, A.; Lewis, J.; Raff, M.; Roberts, K.; Walter, P. *Molecular Biology of the Cell*, 4th ed.; Garland Publishing: New York, 2002.
(14) Kiser, P. F.; Wilson, G.; Needham, D. *Nature* **1998**, *394*, 459.
(15) Karabanova, V. B.; Rogacheva, V. B.; Zezin, A. B.; Kabanov, V. A. *Polym. Sci.* **1995**, *37*, 1138.
(16) Khokhlov, A. R.; Kramarenko, E. Y.; Makhaeva, E. E.; Starodubtzev, S. G. *Macromolecules* **1992**, *25*, 4779.
(17) Khokhlov, A. R.; Kramarenko, E. Y.; Makhaeva, E. E.; Starodoubtzev, S. G. *Makromol. Chem., Theory Simul.* **1992**, *1*, 105.
(18) Hansson, P. *Langmuir* **1998**, *14*, 2269.
(19) Sasaki, S.; Fujimoto, D.; Maeda, H. *Polym. Gels Networks* **1995**, *3*, 145.
(20) Gong, J. P.; Osada, Y. *J. Phys. Chem.* **1995**, *99*, 10971.
(21) Hansson, P. *Langmuir* **1998**, *14*, 4059.
(22) Khandurina, Y. V.; Dembo, A. T.; Rogacheva, V. B.; Zezin, A. B.; Kabanov, V. A. *Polym. Sci.* **1994**, *36*, 189.
(23) Chu, B.; Yeh, F.; Sokolov, E. L.; Starodoubtsev, S. G.; Khokhlov, A. R. *Macromolecules* **1995**, *28*, 8447.
(24) Okuzaki, H.; Osada, Y. *Macromolecules* **1995**, *28*, 380.
(25) Hansson, P. *Langmuir* **2001**, *17*, 4167.
(26) Khandurina, Y. V.; Rogacheva, V. B.; Zezin, A. B.; Kabanov, V. A. *Polym. Sci.* **1994**, *36*, 184.
(27) Hansson, P.; Schneider, S.; Lindman, B. *Prog. Colloid Polym. Sci.* **2000**, *115*, 342.
(28) Hansson, P.; Schneider, S.; Lindman, B. *J. Phys. Chem. B* **2002**, *106*, 9777.
(29) Lynch, I.; Gorelov, A.; Dawson, K. A. *Phys. Chem. Chem. Phys.* **1999**, *1*, 2103.
(30) Matuso, E. S.; Tanaka, T. *J. Chem. Phys.* **1988**, *89*, 1695.
(31) Budtova, T.; Navard, P. *Macromolecules* **1997**, *30*, 6556.
(32) Panyukov, S.; Rabin, Y. *Macromolecules* **1996**, *29*, 8530.
(33) Sekimoto, K. *Phys. Rev. Lett.* **1993**, *70*, 4154.
(34) Sekimoto, K.; Kawasaki, K. *Physica A* **1989**, *154*, 384.
(35) Tomari, T.; Doi, M. *Macromolecules* **1995**, *28*, 8334.
(36) Tanford, C. *Physical Chemistry of Macromolecules*; John Wiley & Sons: New York, 1961.
(37) Manning, G. S. *J. Phys. Chem.* **1969**, *51*, 924.
(38) Hill, T. L. *An Introduction to Statistical Thermodynamics*, 2nd ed.; Addison-Wesley Publishing Co.: Reading, MA, 1962.
(39) Helfferich, F. *Ion Exchange*; McGraw-Hill Book Co., Inc.: New York, 1962.
(40) Fan, L. T.; Singh, S. K. *Controlled Release. A Quantitative Treatment*; Springer-Verlag: Berlin, 1989; Vol. 13.
(41) Coulson, J. M.; Richardson, J. F.; Blackhurst, J. R.; Harker, J. H. *Coulson & Richardson's Chemical Engineering*, 5th ed.; Butterworth-Heinemann: Oxford, 1996; Vol. 1.
(42) Garcia-Mateos, I.; Velazquez, M. M.; Rodriguez, L. J. *Langmuir* **1990**, *6*, 1078.
(43) Hansson, P.; Almgren, M. *J. Phys. Chem.* **1995**, *99*, 16684.
(44) Hayakawa, K.; Santerre, J. P.; Kwak, J. C. T. *Macromolecules* **1983**, *16*, 1642.
(45) Hansson, P.; Almgren, M. *J. Phys. Chem.* **1996**, *100*, 9038.
(46) Oosawa, F. *Polyelectrolytes*; Marcel Dekker: New York, 1971.
(47) Thalberg, K.; Lindman, B.; Bergfeldt, K. *Langmuir* **1991**, *7*, 2893.
(48) Sasaki, S.; Koga, S.; Imabayashi, R.; Maeda, H. *J. Phys. Chem. B* **2001**, *105*, 5852.
(49) Tanaka, T.; Sun, S.; Hirokawa, Y.; Katayama, S.; Kucera, J.; Hirose, Y.; Amiya, T. *Nature* **1987**, *325*, 796.
(50) Cerda, E.; Ravi-Chandar, K.; Mahadevan, L. *Nature* **2002**, *419*, 579.
(51) $D = 4.42 \times 10^{-10}$ m^2/s for DoTAB below cmc in D_2O at 298 K. Prof. Olle Söderman, unpublished data.
(52) Balmbra, R. R.; Clunie, J. S.; Goodman, J. F. *Nature* **1969**, *222*, 1159.
(53) Bull, T.; Lindman, B. *Mol. Cryst. Liq. Cryst.* **1974**, *28*, 155.
(54) Jóhannesson, H.; Halle, B. *J. Chem. Phys.* **1996**, *104*, 6807.
(55) Johansson, L. B.-Å.; Söderman, O. *J. Phys. Chem.* **1987**, *91*, 5275.
(56) Israelachvili, J. N. *Intermolecular and Surface Forces*, 2nd ed.; Academic Press Ltd.: London, 1992.
(57) Hixson, A.; Crowell, J. *Ind. Eng. Chem.* **1931**, *23*, 923.
(58) Manuscript in preparation.
(59) Eichenbaum, G. M.; Kiser, P. F.; Simon, S. A.; Needham, D. *Macromolecules* **1998**, *31*, 5084.
(60) Eichenbaum, G. M.; Kiser, P. F.; Dobrynin, A. V.; Simon, S. A.; Needham, D. *Macromolecules* **1999**, *32*, 4867.
(61) Marszalek, P. E.; Farrell, B.; Verdugo, P.; Fernandez, J. M. *Biophys. J.* **1997**, *73*, 1169.